CrossMark

Highly active palladium nanoparticles immobilized on knitting microporous organic polymers as efficient catalysts for Suzuki–Miyaura cross-coupling reaction

Kunpeng Song[1] · Peng Liu[1] · Jingyu Wang[1] · Bien Tan[2] · Tao Li[1]

Abstract By encaging the Pd nanoparticles in the interior space of the hypercrosslinked microporous organic polymer, we successfully prepared a novel eco-friendly heterogeneous catalyst for Suzuki cross-coupling reaction. The catalyst afforded fast conversions for the Suzuki cross-coupling reaction even at a loading of 0.05 mmol% Pd, and the turnover frequency for the reaction could be up to $61,353 \ h^{-1}$. Furthermore, this catalyst is stable enough to be reused more than five times with no appreciable activity decrease. This work provides a method for fabricating highly active microporous organic polymer encapsulated Pd catalysts for Suzuki cross-coupling reaction and resolve the problem of industrialization in traditional active carbon catalysts.

Keywords Ligand free · Pd catalyst · Microporous organic polymer · Suzuki cross-coupling reaction

✉ Bien Tan
bien.tan@mail.hust.edu.cn

✉ Tao Li
hust_taoli@163.com; taoli@mail.hust.edu.cn

[1] Key Laboratory for Large-Format Battery Materials and System, Ministry of Education, School of Chemistry and Chemical Engineering, Huazhong University of Science and Technology, Luoyu Road No. 1037, Wuhan 430074, China

[2] Institute of Polymer Science and Engineering, School of Chemistry and Chemical Engineering, Huazhong University of Science and Technology, Luoyu Road No. 1037, Wuhan 430074, China

1 Introduction

Palladium catalysed cross-coupling reaction are frequently exploited in modern synthetic chemistry for carbon–carbon bond formation [1–4].Conventional homogeneous catalysts consisting of palladium complexes with a variety of ligands are usually used in these reactions [5–7]. Many excellent studies have been reported on improving the activity and selectivity of these catalysts. However, these homogeneous catalysts are difficult to be operated and recycled, the properties of which make them difficult to be used for chemical process in large scale [8–10].

Heterogeneous catalysts, such as Pd particles or supported Pd composites, are better suited in large-scale practical applications in terms of separation and recycling. A variety of supports, such as polymers [1, 11], metal–organic frameworks (MOFs) [12–14], as well as conventional inorganic material, i.e. active carbon [15, 16], metal oxides [17, 18], silica and zeolites [19], are used to support Pd nanoparticles. However, tedious preparation procedures, relatively low catalytic activity, leaching and aggregation of the Pd species during reactions are generally the issues that need to be addressed [20]. For a practical catalyst, a highly actively heterogeneous Pd catalyst which is also stable enough for multiple recycles is highly desirable.

Currently, MOPs have received significant attention in recent years as a novel class of nanoporous materials mainly due to its possessing various advantages compared to traditional support materials [21–25]. Firstly, their pore structure can be finely tuned by the rigid node-strut topology, in particular by the average strut length [22, 25]. Secondly the surface functionalities can be introduced by a wide variety of synthetic strategies, for example, moieties that could enhance binding affinities or monomers in molecular level [26]. Thirdly, it is well known that most

organic polymers are highly stable to air and water moisture. More importantly, some organic polymers can be synthesized reproducibly from well-defined monomers, although this is often a challenge with activated carbons [27]. MOPs materials as host matrices to support Pd NPs for catalysed C–C coupling reactions have been reported recently [11, 28–30]. It is well known that the size and location of support palladium NPs have an important effect on their catalytic activity and of course the complex microporous structure is beneficial for dispersing Pd NPs [31, 32]. These advantages render MOPs to be potential and possibly superior candidates for the supporter of noble metal catalyst [23].

Nowadays, Suzuki cross-coupling reaction have attracted much attention due to their extensive application in organic synthesis [33], in biology [34], in study of molecular recognition [35] and in design of electron transfer sensors [36]. Because of the great significance of this reaction, it was recognized by rewarding the 2010 Nobel Prize in Chemistry [37]. Most applications of the reaction involve homogeneous catalysts consisting of palladium(II) complexes with a variety of ligands. Theses catalytic systems generally exhibit high activity and selectively than heterogeneous systems, but their industrial applications remained limited due to the difficulty in their separation from the products for recycling [38]. Hence,Owing to the large surface areas and tunable pore size, MOPs are good candidates as catalyst supports for Suzuki reactions. Moreover, polymer supports are popularly recommended by many chemists for their cheapness and high stability in a basic reaction environment. To avoid their leaching and aggregation, palladium species have often been confined in the pore channels or locked in a porous support matrix [39–41]. Generally speaking, the activity of the catalysts is not only determined by the activity species, but also depends on the dispersion and morphology of the palladium. Therefore, if Pd species are embedded in the support, the Palladium cannot diffuse out of the pores of MOPs to form the aggregated nanoparticles on the external surfaces of MOPs and the solution, which would decrease the catalytic activity and reusability of the catalyst. Being smaller in size is expected to increase the nanoparticle surface tension, and for green and sustainable chemistry, MOPs materials with homogeneously dispersed Pd NPs be desirable to overcome the drawbacks of supported palladium catalyst [42]. Hence these MOPs materials applied as heterogeneous Pd nanoparticles catalysts remains a formidable challenge.

In this work, SMP-PhPh$_3$ material incorporating palladium species was synthesized by a strategy previously we have proposed a low-cost strategy to synthesize high surface area HCPs material SMP-PhPh$_3$ [43], and synthesised stable, recoverable and ligand free heterogeneous Pd/SMP-PhPh$_3$ catalyst following a novel strategy. This catalyst enables fast Suzuki–Miyaura coupling reaction in an aqueous ethanol solution under mild conditions. For aryl bromides with both electron-rich and electron deficient substituents, the yield exceeded 90 % after 20 min of reaction at 80 °C and TOF reached about 61,353 h^{-1}. Biaryl products were obtained consistently in excellent yields using various aryl bromides and phenylboronic acid. Moreover this work demonstrates that the MOPs materials can efficiently disperse palladium NPs to promote the catalytic activity, which is much higher than that of homogeneous catalysts under the similar conditions. In this work, we have found one such catalyst with the Pd NPs support on microporous organic polymer (MOPs) prepared with a facile strategy.

2 Experimental

2.1 Materials and methods

All chemicals were purchased from commercial suppliers and used without further purification. HCl, AlCl$_3$ (anhydrous), ethanol and CHCl$_3$ were obtained from National Medicines Corporation Ltd., China, all of which were of analytical grade and were used as received. 1,3,5-triphenylbenzene (sym-PhPh$_3$, Alfa Aesar, 98 %) were also used as received.

2.2 Synthesis of SMP-PhPh$_3$

Under a N$_2$ atmosphere, AlCl$_3$ (2.2 g, 15 mmol) was added to a solution of sym-PhPh$_3$ (0.77 g, 2.5 mmol) in 8 mL CHCl$_3$ with magnetic stirring at 58 °C, and the reaction was allowed to proceed for 48 h at the same temperature under a N$_2$ atmosphere. The resulting precipitate was washed once with ethanol, twice with HCl–H$_2$O (v/v = 2:1), and thrice with ethanol, and finally in a Soxhlet for 24 h with ethanol, and then dried in a vacuum oven at 75 °C for 24 h (pale brown powder, 0.76 g, 99 % yield, C, 77.90 %, H, 4.52 %, Al, 0.030 %). Because AlCl$_3$ is easily hydrolyzed in the presence of water and air to produce HCl, AlCl$_3$ is always accompanied by a small amount of HCl, hence HCl was purposefully not added externally.

2.3 Preparation of Pd/SMP-PhPh$_3$ catalyst

The Pd/SMP-PhPh$_3$ catalyst is prepared through the reduction of the Pd ions in methanol by reflux. The Palladium precursor solution (H$_2$PdCl$_4$) was prepared by adding 10 mg of PdCl$_2$ and 1 ml 0.1 M HCl to a round-bottom flask and the mixture was diluted to about 10 ml with distilled water. A solution containing 10 ml 0.06 mM

of H_2PdCl_4 and 0.2 g of SMP-PhPh$_3$ were prepared. The mixture was kept stirring for 24 h at room temperature. After a reflux treatment with reduction by 10 ml methanol at 70 °C, PdNPs were encapsulated inside the pores of SMP-PhPh$_3$. The resulting solid was isolated by centrifugation, washed with acetone for three times, and then dried at 60 °C under vacuum for 12 h to yield Pd/SMP-PhPh$_3$ as a dark brown-colored powder. The Pd content of the Pd/SMP-PhPh$_3$ catalyst is 0.56 wt% measured by Atomic Absorption Spectroscopy (Perkin Elmer AA-300, American). Catalysed Pd/XC-72 was prepared as the same way, and the Pd content measured by AAS is 0.54 wt%.

2.4 Catalyst preparation and characterization

N$_2$ physical adsorption was carried out on a Micrometrics ASAP 2020 M volumetric adsorption analyzer (before the measurements, samples were degassed at 383 K for 8 h under 10^{-5} bar vacuum). The Brunauer–Emmett–Teller (BET) surface area was evaluated from data in the relative pressure range from 0.05 to 1. The total pore volume of each sample was estimated from the amount adsorbed at the highest P/P$_0$ (above 0.99). Pore diameters were determined from the adsorption branch using Barrett–Joyner–Halenda (BJH) method. Scanning electron microscopy (SEM) images were obtained on a FEI Sirion 200 scanning electron microscope at 10.0 kV. Transmission electron microscopy (TEM) was carried out on a FEI Tecnai G2 20 electron microscope running at 200 kV. The XRD patterns were obtained on a Bruker Advanced D8 diffractometer over a 2θ range of 10°–90° with CuKα radiation. Pd content was analyzed by atomic absorption spectrometry (AAS) on a Perkin Elmer AA-300. The products of the coupling reaction were identified by 1H NMR spectra using a 400 MHz Bruker AV400 instrument in CDCl$_3$. Chemical shifts are reported in parts per million (ppm) downfield from TMS. Field emission scanning electron microscopy (FE-SEM) was performed using a Sirion 200 microscope (FEI Corp., NL) operated at 5 kV. GC analyses were performed in a Fuli GC9790, equipped with a FFAP (30 m × 0.25 mm × 0.25 μm) capillary column and a flame ionization detector (FID).

2.5 Catalytic activity test and recycling

All reactions were conducted in a 10 mL tubular flask equipped with a magnetic stirring bar. In a typical procedure, 10 mg Pd/SMP-PhPh$_3$, 1 mmol bromobenzene, 1.2 mmol phenylboronic acid and 1.5 mmol K$_3$PO$_4$·3H$_2$O were added to 2 ml solvent (EtOH:H$_2$O = 1:1 v/v). The mixture was stirred at 80 °C in air for 5 min. The product was obtained by preparative TLC using petroleum ether as eluting solvent. The product was confirmed by ^{1}H NMR.

For the recycling experiments, 15 mg Pd/SMP-PhPh$_3$, 1 mmol bromobenzene, 1.2 mmol phenylboronic acid, 1.5 mmol K$_3$PO$_4$·3H$_2$O, and 50 mg naphthaline (as internal standard for GC analysis) were added to 2 ml solvent (EtOH:H$_2$O = 1:1 v/v). The reaction was carried out at 80 °C in air for 5 min. Then the mixture was separated quickly by centrifugation. The clear supernatant was analyzed by GC. The obtained catalyst was washed by distilled water and acetone, dried under vacuum for 2 h and used in the next run.

3 Results and discussion

3.1 Characterization of the catalysts

The SEM image (Fig. S1a, b) indicates that the catalyst Pd/SMP-PhPh$_3$ has almost maintained the morphology and structure of SMP-PhPh$_3$, uniform dispersed and abundant porous. As shown in Fig. 1a, smaller Pd nanoparticles were uniformly dispersed on the surface of SMP-PhPh$_3$. The particle size distribution histograms obtained by measuring the sizes of 200 randomly chosen particles (Fig. 1b), the average sizes of the Pd NPs were estimated to about 5.59 nm. HRTEM image (Fig. S2) clearly showed the micropores channels of Pd/SMP-PhPh$_3$, and further confirmed the crystalline nature of Pd nanoparticles and lattice spacing of 0.224 nm, corresponding to the inter planar spacing of Pd (111) [44]. We also compared the TEM images of Pd/XC-72 (Fig. 1c, d), the dispersion of Pd NPs is not uniformly and the diameter is about 9.29 nm. From the TEM image it can be seen that the size of Pd NPs on SMP-PhPh$_3$ is uniform distributed and smaller than active carbon. We conclude that the abundant micrporous structures have a well dispersion of Pd precursor, the Pd NPs were embedded in the internal micropores and it prevents the growing up of Pd NPs in the reduction process. And we can directly observe that the palladium particles were covered by organic layers (Fig. S2). Based on this design conception, we expect Pd NPs can be restricted in pores and keep good stability during reaction.

Figure 2a is the X-ray diffraction pattern of the Pd@SMP-PhPh$_3$ catalyst, in which the peak located at 40.1 can be assigned to the (111) plane of Pd (0) (JCPDS: 65-6174) (Fig. 2b); the peak intensity weaker than that of Pd/XC-72 (Fig. S3), because other reflections of Pd(0) embedded in internal are difficult to be recognized in the diffraction pattern. And the Pd NPs embedded in SMP-PhPh$_3$ is smaller and more homogeneous.

The XPS spectra (Fig. S4) demonstrate that the Pd species in the sample Pd/SMP-PhPh$_3$ was present in the metallic state with the bond energy about 335.8 and 341.7 eV in the Pd 3d$_{5/2}$ and Pd 3d$_{3/2}$ core level.
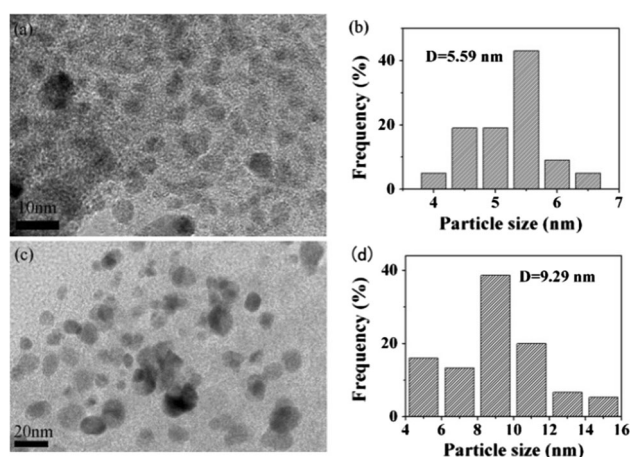
Fig. 1 The TEM images and particles size distribution of catalyst Pd/SMP-PhPh$_3$ (**a**, **b**) and Pd/XC-72 (**c**, **d**)
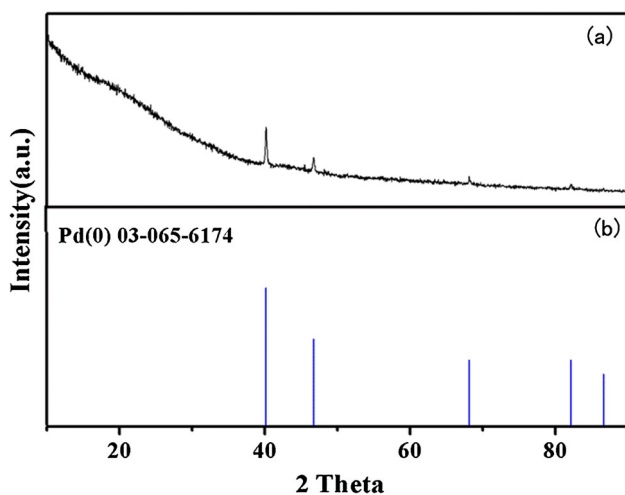

Fig. 2 XRD patterns of catalyst Pd/SMP-PhPh$_3$ (**a**) and PDF stand card of Pd(0) (**b**)

Nitrogen sorption experiments were conducted to investigate the porous structure of the sample. As presented in Fig. 3a, the sorption isotherm of Pd/SMP-PhPh$_3$ is very similar to that of pristine SMP-PhPh$_3$ which indicates that the insertion of Pd species has not destroyed the porous state. The typical type I curve with a steep uptake at low relative pressures below 0.001 reveal the abundant micropores, the main size of the micopores in Pd/SMP-PhPh$_3$ was around 0.6 nm determined by the Barrett–Joyner–Halenda (BJH) poresize distribution (Fig. 3b). But the BET surface area and pore volume of Pd/SMP-PhPh$_3$ ($\sim$1068 m^2 g^{-1}, 0.56 cm^3 g^{-1}) are lower than that of SMP-PhPh$_3$ ($\sim$1254 m^2 g^{-1}, 0.66 cm^3 g^{-1}). This reflects the fact that Pd species have been indeed embedded in SMP-PhPh$_3$.
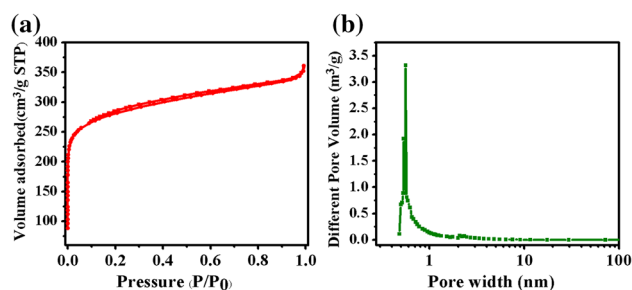

Fig. 3 Nitrogen adsorption–desorption isotherms (**a**) and pore size distribution curves (**b**) for Pd/SMP-PhPh$_3$

3.2 The Suzuki–Miyaura cross-coupling reaction

We first tested the catalytic activity of Pd/SMP-PhPh3 in the Suzuki cross-coupling reaction between bromobenzene and phenylboronic acid, and the result are summarized in Table 1. Previous studies have showed that solvents and bases had remarkable influences on the activity of the Suzuki reaction [45]. And our interest is using water to replace organic solvents in such reaction because water solvent endows the reaction with green and safe properties [46, 47]. But, we can only get 50 % yield in water though the result is better than other organic solvents (Table 1, entries 1–6) at the same reaction condition.

When ethanol was test as the solvents, the reaction yield can reach 95 %. (Table 1, entry 7) Our preliminary research revealed that the presence of ethanol could efficiently promote the Suzuki–Miyaura reaction in water (Table 1, entries 8–10). And the optimal condition was using with K$_3$PO$_4$·3H$_2$O as base and 50 % aqueous ethanol was the best choice for the reaction medium (Table 1, entry 9). Under the same conditions, Na$_2$CO$_3$, K$_2$CO$_3$, NaPO$_4$·12H$_2$O, KOt-Bu, NaOAc and NaOH gave moderate biphenyl yield (Table 1, entries 11–16). Remarkably, when K$_3$PO$_4$·3H$_2$O and Na$_3$PO$_4$·12H$_2$O were used (Table 1, entries 9 and 11), excellent biphenyl yields were obtained, illustrates stronger base can efficiently promote Suzuki reaction.

Indeed, K$_3$PO$_4$·3H$_2$O in 50 % aqueous ethanol was found to be the best choice in view of almost quantitative biphenyl yield obtained within considerably short reaction time (5 min) (Table 1, entry 9). A reaction catalysed by 1 mg catalyst was also carried out, and it was found that the reaction proceeded uneventfully, which indicated the effectiveness of this catalyst for practical synthesis (Table 1, entry 9^c).

After the optimized of solvent and base, we compared the catalytic activity of several solid catalysts. At the same reaction condition and Pd content, the catalysts Pd/SMP-PhPh$_3$ and Pd/XC-72 give the highest yields (Table 2, entries 1–2). However, the commercial Pd/C only have

Table 1 The effect of bases and solvents[a]

Entry	Solvents	Base	Time (min)	Yield[b] (%)
1	H_2O	$K_3PO_4 \cdot 3H_2O$	5	50
2	DMF	$K_3PO_4 \cdot 3H_2O$	5	16
3	CH_3CN	$K_3PO_4 \cdot 3H_2O$	5	6
4	toluene	$K_3PO_4 \cdot 3H_2O$	5	13
5	dioxane	$K_3PO_4 \cdot 3H_2O$	5	17
6	cyclohexane	$K_3PO_4 \cdot 3H_2O$	5	33
7	EtOH	$K_3PO_4 \cdot 3H_2O$	5	95
8	EtOH/H_2O(2:1)	$K_3PO_4 \cdot 3H_2O$	5	99
9	EtOH/H_2O(1:1)	$K_3PO_4 \cdot 3H_2O$	5	100 (99)[c]
10	EtOH/H_2O(1:2)	$K_3PO_4 \cdot 3H_2O$	5	99
11	EtOH/H_2O(1:1)	$NaPO_4 \cdot 12H_2O$	5	99
12	EtOH/H_2O(1:1)	Na_2CO_3	5	98
13	EtOH/H_2O(1:1)	K_2CO_3	5	95
14	EtOH/H_2O(1:1)	KOt-Bu	5	99
15	EtOH/H_2O(1:1)	CH_3COONa	5	49
16	EtOH/H_2O(1:1)	NaOH	5	63

[a] Reaction condition: bromobenzene (0.5 mmol), phenylboronicacid (0.75 mmol), base (1.5 mmol), solvent (2 mL), 80 °C, Pd/SMP-PhPh₃10 mg
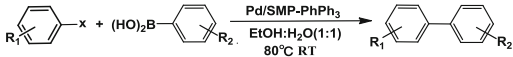
[b] Isolate yield

[c] 1 mg catalyst

Table 2 The catalytic activity comparison of different solid catalysts
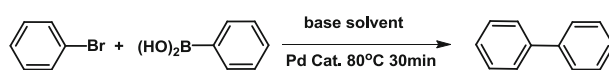
Entry	Catalyst	Yield (%)	Pd (wt%)
1	Pd/SMP-PhPh₃	99	0.56
2	Pd/XC-72	99	0.54
3	Commercial Pd/C	95	5
4	Pd/SiO₂	64	0.42
5	Pd/Al₂O₃	73	0.47

Reaction conditions: bromobenzene (1 mmol), phenylboronicacid (1.2 mmol), $K_3PO_4 \cdot 3H_2O$ (1.5 mmol), solvent (EtOH: H_2O = 1:1, 2 mL), 80 °C, 30 min and at a Pd loading of 0.05 mmol%

95 % yield (Table 2, entry 3). The traditional inorganic support, such as Pd/SiO₂ and Pd/Al₂O₃ give a yield of 64 and 73 %, respectively (Table 2, entries 4–5). From the Table 2 we clearly find the Pd loading of prepared catalysts is Pd/SMP-PhPh₃ > Pd/XC-72 > Pd/Al₂O₃Pd/SiO₂, we think the high surface area and porosity MOPs is benefit to immobilized the Pd NPs and prevent it from leaching during the reaction, and also the rich in microporous of MOPs is conducive to get smaller and uniform Pd NPs (Fig. 1). It is the reason why Pd/SMP-PhPh₃ gave the highest yield and well cyclical.

With the optimized solvent and base in hand, we investigated the activity of Pd/SMP-PhPh₃ for various substrates. All the reactions were carried out at 80 °C in air using a 50 % aqueous ethanol solution as a reaction medium. The results are summarized in Table 3. At the Pd loading of 0.05 mmol %, Pd/SMP-PhPh₃ afford satisfactory biaryl yields (95–99 %) for halogen-benzenes containing –OCH₃ and –CN groups within 5–20 min (Table 3, entries 1–3). It is worth to note that the TOF reached ca.61,353 h⁻¹ in the case of bromobenzene. For iodobenzene and other aryl iodides with substituents such as –CH₃

Table 3 Pd/SMP-PhPh₃catalysed Suzuki coupling reaction[a]

$$R_1 \overset{}{\bigcirc}-X \ + \ (HO)_2B-\bigcirc R_2 \xrightarrow[\substack{EtOH:H_2O(1:1)\\80°C\ RT}]{Pd/SMP-PhPh_3} \ R_1\overset{}{\bigcirc}-\bigcirc R_2$$

Entry	ArX	ArB(OH)₂	Time	Yield	TOF
			min	(%)	(h⁻¹)
1	◯–Br	(HO)₂B–◯	5	99	61353
2	H₃CO–◯–Br	(HO)₂B–◯	5	99	49054
3	NC–◯–Br	(HO)₂B–◯	20	95	14472
4	◯–I	(HO)₂B–◯	5	99	24494
5	–◯–I	(HO)₂B–◯	15	90	11208
6	◯–Br	(HO)₂B–◯–	10	96	11819
7	◯–Br	(HO)₂B–◯–	20	90	11887
8	◯–Br	(HO)₂B–◯	20	87	11811
9	◯–Br	(HO)₂B–◯–OCH₃	10	98	26608
10	◯–Br	(HO)₂B–◯–Cl	10	93	10068
11	◯–Br	(HO)₂B–◯◯	15	99	9280
12	◯–Br	(HO)₂B–◯–OCF₃	25	90	5020
13	◯ₙ–Br	(HO)₂B–◯	180	50	642

[a] Reaction condition: aryl halides (0.5 mmol), phenylboronic acid (0.75 mmol), base (1.5 mmol), EtOH-H₂O (V/V = 1:1, 2 ml)

Fig. 4 **a** Reuse of Pd/SMP-PhPh₃ and Pd/XC-72 catalysts for Suzuki–Miyaura coupling reaction, **b** Suzuki–Miyaura coupling reaction in the presence of the filtrate

total TON (turnover numbers) for 5 cycles was up to 25,800.

However, the recycling results showed that the catalytic activity of Pd/XC-72 decreased quickly in the second and the third run (65 and 35 %, respectively). This is probably due to the aggregation and loss of most PdNPs from the surface of active carbon. And the TEM image of the reused Pd/SMP-PhPh₃ (Fig. S5) also is consistent with the experiment result, after runs, Pd NPs in SMP-PhPh₃ still have a small size and uniform distribution. ICP analysis showed that the Pd content in the catalyst Pd/SMP-PhPh₃ after 5 cycles in 0.53 wt% (compared with 0.56 wt% in the fresh catalyst), showing that only a trace of Pd had been lost during the reaction. While in Pd/XC-72 is only 0.18 wt% after 5 cycles (compared with 0.54 wt% in the fresh). Undoubtedly, this result is very promising and encouraging from a practical point of view.

It is interesting to investigate whether the coupling reaction catalysed by Pd/SMP-PhPh₃ or the leached homogeneous Pd species. First, Pd/SMP-PhPh₃ was dispersed in aqueous-ethanol (v: v = 1:1) solvent with K₃PO₄·3H₂O via sonication for 5 min, followed by filtration to remove the solid catalyst. The corresponding amount of bromobenzene and phenylboronic acid was then added to the filtrate with stirring and no biphenyl was detected even after 60 min (Fig. 4b). The superior catalytic activity of Pd/SMP-PhPh₃ observed here can be attributed to the specific characteristics of pore structures of SMP-PhPh₃ and Pd NPs. The π–π conjugated structure of support has plenty of anchor sites for the Pd atoms, which is in favor to disperse and stabilize the Pd NPs. And the complex pore structure can prevent the Pd NPs from leaching during the reaction process.

and –OCH₃, complete conversions of them were observed and the corresponding biaryl products in 92–99 % yields were also achieved within 10 min–15 min (Table 3, entries 4–6). We further tested the catalytic performances for the couplings of various arylboronic acids with bromobenzene (Table 3, entry 7–12). For arylboronic acids bearing electron-donating group –OCH₃ and electron-withdrawing group –CF₃ and –Cl, 86, 83 and 88 % yields were obtained, respectively. Even the 1-naphthyl phenyl boric acid can get a 99 % yield in 15 min. It is noteworthy that sterically hinder phenylboronic acid with *o*-substituted –CH₃, can also easily be converted with 87 % yields. Further study indicated that 2-Bromopyridine can also react with phenylboronic acid, however, the yield of biphenyl was very poor (50 %) even prolonged the reaction time (180 min) (Table 3, entry 13).

The recyclability of Pd/SMP-PhPh₃ and Pd/XC-72 were also investigated with consecutive Suzuki cross-coupling reaction of bromobenzene with phenylboronic acid (Fig. 4a). The catalyst Pd/SMP-PhPh₃ could be recycled 5 times without obvious loss of activity. The average yield of biphenyl in consecutive reactions promoted by the 1st through to the 5th recycled catalyst was up to 97 % and the
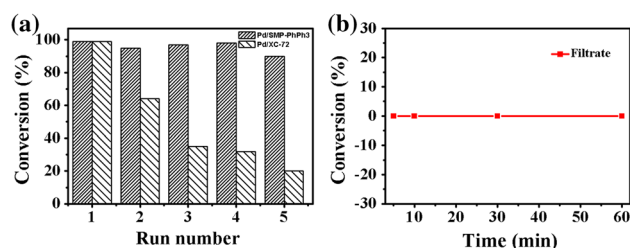
4 Conclusions

By encaging the PdNPs in the interior space of SMP-PhPh₃, a novel and ligand free solid palladium catalyst Pd/SMP-PhPh₃ was successfully prepared. The catalyst affords fast conversions for the Suzuki–Miyaura cross-

coupling reactions of various aryl halides and arylboronic acids even at catalyst loading of 0.05 mmol% in aqueous media. The TOF could be up to 61,353 h^{-1} under mild conditions in air. In particularly, because of the post-cross-coupling network structure, Pd/SMP-PhPh$_3$ shows outstanding stability and reusability can be reused at least 5 times. In addition, the developed solid catalyst exhibits superior substrate selectivity in a mixed system for practical synthesis.

References

1. P. Cotugno, M. Casiello, A. Nacci, P. Mastrorilli, M.M. Dell'Anna, A. Monopoli, J. Organomet. Chem. **752**, 1–5 (2014)
2. V. Ritleng, C. Sirlin, M. Pfeffer, Chem. Rev. **102**, 1731–1770 (2002)
3. R.B. Bedford, C.S. Cazin, D. Holder, Coord. Chem. Rev. **248**, 2283–2321 (2004)
4. R. Barroso, R.A. Valencia, M.-P. Cabal, C. Valdes, Org. Lett. **16**, 2264–2267 (2014)
5. D.P. Hruszkewycz, D. Balcells, L.M. Guard, N. Hazari, M. Tilset, J. Am. Chem. Soc. **136**, 7300–7316 (2014)
6. R. Rossi, F. Bellina, M. Lessi, C. Manzini, G. Marianetti, L.A. Perego, Curr. Org. Chem. **19**, 1302–1409 (2015)
7. J.C. Shi, Z. Zhou, S. Zheng, Q. Zhang, L. Jia, J. Lin, Tetrahedron Lett. **55**, 2904–2907 (2014)
8. D.J. Snelders, G. van Koten, R.J. Klein, Gebbink. J. Am. Chem. Soc. **131**, 11407–11416 (2009)
9. W. Tang, A.G. Capacci, X. Wei, W. Li, A. White, N.D. Patel et al., Angew. Chem. **122**, 6015–6019 (2010)
10. R. Martin, S.L. Buchwald, Acc. Chem. Res. **41**, 1461–1473 (2008)
11. Q. Wen, T.Y. Zhou, Q.L. Zhao, J. Fu, Z. Ma, X. Zhao, Macromol. Rapid Commun. **36**, 413–418 (2015)
12. N. Shang, S. Gao, X. Zhou, C. Feng, Z. Wang, C. Wang, RSC Adv. **4**, 54487–54493 (2014)
13. P. Puthiaraj, W.-S. Ahn, Catal. Commun. **65**, 91–95 (2015)
14. A.S. Roy, J. Mondal, B. Banerjee, P. Mondal, A. Bhaumik, S.M. Islam, Appl. Catal. A Gen. **469**, 320–327 (2014)
15. C. Liu, X. Rao, Y. Zhang, X. Li, J. Qiu, Z. Jin, Eur. J. Org. Chem. **2013**, 4345–4350 (2013)
16. W. Tang, J. Li, X. Jin, J. Sun, J. Huang, R. Li, Catal. Commun. **43**, 75–78 (2014)
17. B. Karimi, F. Mansouri, H. Vali, Green Chem. **16**, 2587–2596 (2014)
18. K.S. Prasad, H.-B. Noh, S.S. Reddy, A.E. Reddy, Y.-B. Shim, Appl. Catal. A Gen. **476**, 72–77 (2014)
19. C. Liu, Z. Shao, Z. Xiao, C.T. Williams, C. Liang, Energy Fuels **26**, 4205–4211 (2012)
20. N. Polystyrene-Supported, H.C.P.C.T. Kang, Q. Feng, M. Luo, Synlett **2005**, 2305–2308 (2005)
21. A.I. Cooper, Adv. Mater. **21**, 1291–1295 (2009)
22. J.-X. Jiang, F. Su, A. Trewin, C.D. Wood, N.L. Campbell, H. Niu et al., Angew. Chem. Int. Ed. **46**, 8574–8578 (2007)
23. B. Li, Z. Guan, W. Wang, X. Yang, J. Hu, B. Tan et al., Adv. Mater. **24**, 3390–3395 (2012)
24. J.X. Jiang, A.I. Cooper, Top. Curr. Chem. **293**, 1–33 (2009)
25. J.-X. Jiang, F. Su, A. Trewin, C.D. Wood, H. Niu, J.T.A. Jones et al., J. Am. Chem. Soc. **130**, 7710–7720 (2008)
26. M. Karbarz, K. Pyrzynska, J. Romanski, J. Jurczak, Z. Stojek, Polymer **51**, 2959–2964 (2010)
27. B. Li, R. Gong, W. Wang, X. Huang, W. Zhang, H. Li et al., Macromolecules **44**, 2410–2414 (2011)
28. S. Xu, K. Song, T. Li, B. Tan, J. Mater. Chem. A. **3**, 1272–1278 (2015)
29. Y. Zhang, G. Ni, C. Li, S. Xu, Z. Zhang, X. Xie, Tetrahedron **71**, 4927–4932 (2015)
30. T. Ratvijitvech, R. Dawson, A. Laybourn, Y.Z. Khimyak, D.J. Adams, A.I. Cooper, Polymer **55**, 321–325 (2014)
31. Z. Wang, W. Chen, Z. Han, J. Zhu, N. Lu, Y. Yang et al., Nano Res. **7**, 1254–1262 (2014)
32. S.I. Yamamoto, H. Kinoshita, H. Hashimoto, Y. Nishina, Nanoscale. **6**, 6501–6505 (2014)
33. A. Suzuki, J. Organomet. Chem. **576**, 147–168 (1999)
34. A.H. Soloway, W. Tjarks, B.A. Barnum, F.-G. Rong, R.F. Barth, I.M. Codogni et al., Chem. Rev. **98**, 1515–1562 (1998)
35. G. Wulff, B. Heide, G. Helfmeier, J. Am. Chem. Soc. **108**, 1089–1091 (1986)
36. T.D. James, P. Linnane, S. Shinkai, Chem. Commun. 281–288 (1996)
37. X.F. Wu, P. Anbarasan, H. Neumann, M. Beller, Angew. Chem. Int. Ed. **49**, 9047–9050 (2010)
38. B. Yuan, Y. Pan, Y. Li, B. Yin, H. Jiang, Angew. Chem. Int. Ed. **49**, 4054–4058 (2010)
39. Y. Ji, S. Jain, R.J. Davis, J. Phys. Chem. B. **109**, 17232–17238 (2005)
40. G. Budroni, A. Corma, H. García, A. Primo, J. Catal. **251**, 345–353 (2007)
41. M.B. Thathagar, J.E. ten Elshof, G. Rothenberg, Angew. Chem. Int. Ed. **45**, 2886–2890 (2006)
42. H. Zhang, Y. Yang, W. Dai, D. Yang, S. Lu, Y. Ji, Catal. Sci. Technol. **2**, 1319–1323 (2012)
43. B. Li, Z. Guan, X. Yang, W.D. Wang, W. Wang, I. Hussain et al., J. Mater. Chem. A. **2**, 11930 (2014)
44. J. Sun, Y. Fu, G. He, X. Sun, X. Wang, Catal. Sci. Technol. **4**, 1742–1748 (2014)
45. R. Kardanpour, S. Tangestaninejad, V. Mirkhani, M. Moghadam, I. Mohammadpoor-Baltork, A.R. Khosropour et al., J. Organomet. Chem. **761**, 127–133 (2014)
46. I. Hoffmann, B. Blumenroder, S.O. nee Thumann, S. Dommer, J. Schatz, Green Chem. **17**, 3844–3857 (2015)
47. R. Zhong, A. Pöthig, Y. Feng, K. Riener, W.A. Herrmann, F.E. Kühn, Green Chem. **16**, 4955–4962 (2014)